# Rheological and Dielectric Behavior of Dipole-Inverted $(SIS)_p$-Type Multiblock Copolymers: Estimates of Bridge/Loop Fractions for Respective I Blocks and Effect of Loops on High Extensibility of Bridges

**Hiroshi Watanabe,* Yumi Matsumiya, Toshiaki Sawada, and Tatsuya Iwamoto**

*Institute for Chemical Research, Kyoto University, Uji, Kyoto 611-0011, Japan*

*Received June 5, 2007; Revised Manuscript Received July 7, 2007*

ABSTRACT: A series of symmetric styrene− (S−) *cis*-isoprene (I) multiblock copolymers of $(SIS)_p$-type ($p$ = 1, 2, 3, and 5 corresponding to tri-, penta-, hepta-, and undecablock) was synthesized with an anion-coupling method and their rheological and dielectric behavior was examined in *n*-tetradecane (C14), a solvent dissolving the I block and precipitating the S block. The molecular weights of the constituent blocks were almost identical for these copolymers, and a particular I block(s) of respective copolymers had symmetrically once-inverted type-A dipole while the remaining I blocks had noninverted dipoles. At 20 °C, the $(SIS)_p$/C14 systems with the $(SIS)_p$ concentration of 40 wt % formed a bcc lattice of glassy, spherical S domains (as confirmed from SAXS) and exhibited the gel-like elasticity. This elasticity was sustained mainly by the bridge-type I blocks connecting the S domains and partly by the coexisting loop-type I blocks. The dielectric loss ($\epsilon''$) data exclusively detected the fluctuation of the midpoint of the dipole-inverted I block having either bridge or loop conformation. (Since the ends of the I blocks were immobilized on the surface of the glassy S domains, the motion of the I blocks having noninverted dipoles was dielectrically inert.) A moderate difference was noted for the $\epsilon''$ data of the $(SIS)_p$ copolymers normalized by the volume fractions of respective dipole-inverted I blocks. This difference unequivocally indicated that the bridge- and loop-type I blocks exhibited different dielectric responses and that the bridge fraction $\phi_{bridge}$ moderately changed with the location of the dipole-inverted I block in the $(SIS)_p$ copolymer backbone as well as the number of repeating SIS units, $p$. On the basis of a hypothesis of dielectric similarity between the loop and its half-fragment tail under an osmotic constraint, $\phi_{bridge}$ was estimated from the $\epsilon''$ data of the $(SIS)_p$ copolymers and their precursor SI diblock copolymer (having the tail-type I block). $\phi_{bridge}$ was a little larger for the I block located at the center of the copolymer backbone than for the off-center I block and $\phi_{bridge}$ of the center I block decreased slightly with increasing $p$. The $(SIS)_5$ undecablock system was extensible up to the stretch ratio of $\lambda \cong 30$, and the loops therein appeared to osmotically stretch the bridges thereby helping the bridges bear such a high extensibility.

## 1. Introduction

Microdomain structures and properties of block copolymers have been one of the most interesting subjects in the field of polymer physics.[1] For the simplest A−B diblock copolymers having the tail-type conformation in both of the A and B blocks, extensive studies[1−4] have been made for the thermodynamics, the microdomain and grain structures, and the dynamics of the respective blocks.[1−4]

Studies have been extended to A−B−A triblock copolymers having either bridge or loop conformations in the middle B block. The microdomain structure is similar for A−B diblock and their head-to-head dimer, $A-B_2-A$ triblock copolymers,[2,5−7] and the mechanical properties are also similar *for some cases*. For example, a styrene− (S−) *cis*-isoprene (I) diblock copolymer and its dimer (SIS triblock copolymer) dissolved in *n*-tetradecane (C14; an I-selective solvent precipitating the S block) form almost identical bcc lattices of glassy S domains to exhibit nearly the same equilibrium modulus when the copolymers are rather dilute and the I blocks are not entangled among themselves.[8] For this case, the tail-type I block of SI and the loop-type I block of SIS are subjected to an osmotic constraint of maintaining the uniform concentration distribution thereby sustaining the equilibrium modulus.[8−11] Their modulus is similar, in magnitude, to that of the nonentangled bridge-type I blocks subjected to the same constraint.[8]

* To whom correspondence should be addressed.

However, for most cases, significant differences are noted for mechanical properties of the triblock and diblock copolymers. The equilibrium modulus sustained by a bridge-type high-*M* block in bulk is larger than that of a corresponding loop-type block, as demonstrated from experiments for blends of A−B−A-type triblock, A−B−C type triblock forming only B-bridges, and A−B type ring diblock forming only A- and B-loops.[12,13] This difference of the modulus is attributable to the trapped entanglements (knots) formed by the high-*M* blocks.[12]

Even more striking differences are noted for the nonlinear mechanical behavior. Under flow, SI diblock systems forming a lattice of spherical S domains exhibit the simple plastic behavior without the chain pullout process (because the tail-type I blocks therein do not bridge the S domains).[9−11] The yield stress of this system reflects the thermodynamic stability of the lattice. In contrast, the SIS system exhibits significant yielding at high temperatures where the S domains are in the liquid state. This behavior is associated with the pullout of the S blocks connected to the bridge-type I block, and the yield stress reflects, at least partly, the thermodynamic penalty of S/I mixing.[14,15] The yielding is observed also for lamellar SIS triblock and SI diblock systems having glassy S domains, and the role of bridge-type blocks has been discussed.[16,17]

The study of the loop/bridge problem has been extended to linear *multiblock* copolymers of $(ABA)_p$- and $(AB)_p$-types,[7,16−23]

10.1021/ma0712495 CCC: $37.00 
Published on Web 08/21/2007

the former having A blocks at both ends and the latter having A and B blocks at respective ends. For a series of copolymers having an almost identical molecular weight for all blocks, several groups[7,16,21] have reported moderate changes of the microdomain size with the repeating unit number $p$ and discussed a consistency with the self-consistent mean field (SCF) theory. For a lamellar-forming S{ISISISISI}S undecablock copolymer having long S blocks at both ends, Matsushita and co-workers[22] found that the inner nonablock part forms only three-layer lamella because of a strong influence of the outer S blocks on the conformation of the inner part.

The number of the repeating unit, $p$, strongly affects mechanical properties. For example, the yield strength of S/I lamellae of the $(SIS)_p$- and $(SI)_p$-type multiblock copolymers increases with increasing $p$ possibly due to an enhancement of the strength sustained by the bridges.[16,17] Bates et al.[7,17−20] further examined the effect of shear on the bridge formation in the S/I multiblock lamella: The bridge formation is moderately enhanced for the shear-orientated perpendicular lamella but significantly suppressed for the parallel lamella, as evidenced from a lamellar delamination test in an I-selective solvent (tetradecane). This fact suggests that the bridges crossing the flow plane (velocity−vorticity plane) is converted to the loops, as deduced also from a recent theory.[23]

For the copolymers composed of finite number of blocks ($\leq$11 so far examined), all blocks are not necessarily equivalent and the bridge fraction may change according to the block location in the copolymer backbone. It is interesting to evaluate the bridge fractions for *respective* blocks and examine the contribution of respective bridges to the mechanical properties. Nevertheless, none of studies so far conducted gave an estimate even for an average bridge fraction.

This study attempts to experimentally estimate the bridge faction and examine its dependence on the total block number as well as the block location in the copolymer backbone. For A−B−A triblock copolymers having only one type of inner B block, the estimate may be made with viscoelastic,[12] swelling,[24] and dielectric[8,25,26] methods on the basis of respective assumptions. In particular, the dielectric method gave an estimate close to the SCF prediction.[27,28] For our target of estimating the bridge fraction for a particular block(s) in the multiblock copolymers, the best available method seems to be the dielectric method with the following strategy: We focus on $(SIS)_p$-type symmetric multiblock copolymers at low temperatures where the S domains are in the glassy state. The I block has the so-called type-A dipole parallel along the backbone, and its slow dielectric relaxation is activated only by the end-to-end vector fluctuation *if* the dipole is not inverted in the block.[10,29] Consequently, at low temperatures where the ends of all I blocks are immobilized on the surface of glassy S domains, the I blocks having no dipole-inversion give no dielectric signal in long time scales. In contrast, if the dipole is symmetrically once-inverted in a particular I block, the midpoint fluctuation of this block activates the slow dielectric relaxation.[8,10,25] Thus, we can introduce the dielectric label (=inversion) for a desired I block and selectively observe the dielectric signal from this block. On the basis of the hypothesis of dielectric similarity of a dipole-inverted loop-type I block and a tail-type I block,[8,25] the latter being equivalent to a half-fragment of the former, we can compare the dielectric data for the $(SIS)_p$-type multiblock copolymer (having the dipole-inverted I block) and a corresponding SI diblock copolymer to estimate the bridge fraction for the former.

For SIS triblock copolymers, this hypothesis gave the estimate close to the SCF prediction.[8,25] The hypothesis is consistent with an experimental result that the dielectric data are very similar for the SI diblock copolymer and its dimer (SIS triblock copolymer) at low concentrations where the bridge should be stretched/destabilized and the loop should become the dominant component in the SIS system.[8] The hypothesis is also consistent with the other result that the dielectric data of SIS hardly change on blending with SI:[26] Within the hypothesis, the blending is equivalent to an addition of loops to the SIS system, and the reequilibration of SIS conformation can keep the same bridge/(loop+tail) ratio to give the same dielectric data.

Despite these experimental supports, the hypothesis has not been justified from the first principle of the dynamics of osmotically constrained block chains (which itself is awaited to be fully established), and the bridge fraction thus obtained is to be regarded as a *rough estimate*.[8,10,25] This estimate is to be replaced by a more accurate result obtained from an absolute method such as small-angle neutron scattering (SANS) for the multiblock copolymers selectively deuterated for a particular block(s). However, no such result is available at this moment. Wu and co-workers[20] correctly criticized the uncertainty in the dielectric method and explained the superiority of the SANS method, but they reported no bridge fraction evaluated from their SANS data. In this situation, the dielectric estimate appears to be the best available estimate at this moment.

Thus, we synthesized a series of symmetric tri-, penta-, hepta-, and undecablock copolymers of $(SIS)_p$-type ($p$-mer of SIS) having almost identical molecular weights of the constituent blocks and the dipole inversion in a particular I block(s) and examined their dielectric and rheological behavior. The dielectric data suggested that the bridge fraction $\phi_{bridge}$ of the center I block of the heptablock copolymer is larger than that of the off-center I block and that $\phi_{bridge}$ of the center I block decreases slightly with an increase of the number of repeating SIS unit, $p$. This paper presents details of these results and further discusses the high extensibility of the $(SIS)_p$ systems in relation to an osmotic stretching of the bridges due to the coexisting loops.

## 2. Experimental Section

**2.1. Synthesis of Materials.** A series of symmetric styrene−(S−) *cis*-isoprene (I) multiblock copolymers of $(SIS)_p$-type (having the S blocks at both ends) was synthesized via stepwise living anionic polymerization followed by anionic coupling.[30] The synthesis was made with a standard high vacuum technique utilizing glass flasks/ampules, constrictions, and breakable seals.[31−33] The polymerization solvent was benzene, and the initiator was *sec*-butyllithium (synthesized from *sec*-butyl chloride and Li metal in heptane). All chemicals were purchased from Wako Co. Ltd. and purified with standard methods.[31−33]

The route of the stepwise polymerization of the copolymer samples is shown in Scheme 1. After each step of polymerization, the precursor was recovered for convenience of characterizing the samples.

First, $S^-$ anion was polymerized with *sec*-butyllithium in benzene and split into two mother batches. The $S^-$ anion in the first mother batch was copolymerized with I monomer, and the resulting $SI^-$ anion was split into three daughter batches; see the top part of Scheme 1.

The $SI^-$ anion in the first daughter batch was terminated with methanol (MeOH) to recover the SI diblock sample. The $SI^-$ anion in the second batch was allowed to react with equimolar bifunctional coupler, 1,4-bis(chloromethyl)benzene (bCMB) diluted with tetrahydrofuran (THF), to give the $SI_2S$ triblock sample having the symmetrically once-inverted type-A dipole in the middle $I_2$ block, as done in the previous work for synthesis of symmetrically dipole-inverted homopolyisoprenes:[30,34] Hereafter, "$I_2$" stands for the I block having the inverted dipole. The crude product was repeatedly

**Scheme 1. Synthetic Route of the $(SIS)_p$ Multiblock Copolymer Samples**

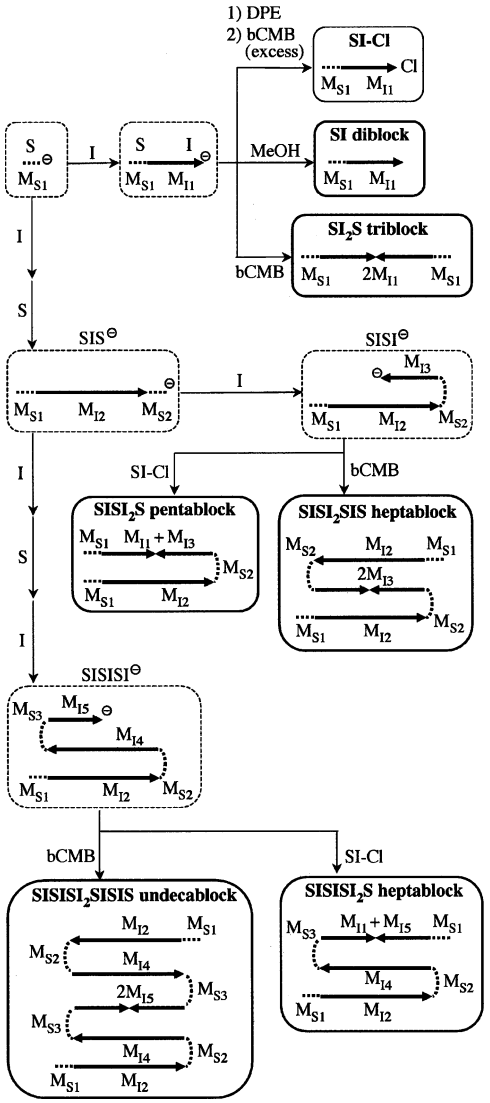


fractionated from benzene/methanol mixtures to recover the $SI_2S$ triblock sample. (The coupling with bis(halomethyl)benzene was utilized also by Wu and co-workers to synthesize symmetric multiblock copolymers but they made no fractionation.[7])

The $SI^-$ anion in the third daughter batch was allowed to react with 1,1-diphenyl ethylene (to convert the isoprenyl anion to less reactive diphenyl ethylenyl anion) and then with ~100 times excess of bCMB dissolved in THF. The SI polymer end-capped with the chloromethylbenzene group (SI−Cl) was successfully obtained from this reaction. The crude product was precipitated in acetone to remove unreacted bCMB, and the precipitant recovered by decantation was dissolved in benzene. After this precipitation/dissolution process repeated for three times in vacuum, the SI−Cl polymer was thoroughly dried in high vacuum, dissolved in benzene, and recovered in separate ampules. This end-chlorinated polymer was utilized as a macromolecular end-capping agent in the coupling reaction described below.

The $S^-$ anion in the second mother batch was copolymerized with I monomer and then with S monomer to give the $SIS^-$ prepolymer anion; see the middle part of Scheme 1. This $SIS^-$ anion was split into two batches, and the anion in one batch was copolymerized with I monomer to give $SISI^-$ anion. This $SISI^-$ anion was further split into two batches and allowed to react with equimolar macromolecular end-capping agent, SI−Cl, or bifunctional coupler, bCMB. The crude products of these two batches were repeatedly fractionated from benzene/methanol mixtures to recover the $SISI_2S$ pentablock and $SISI_2SIS$ heptablock samples.

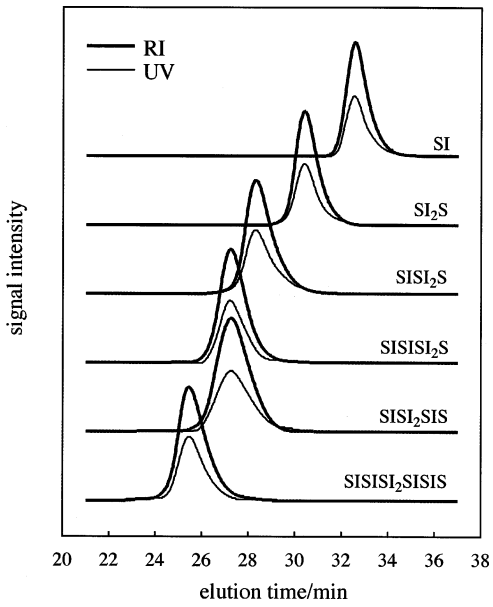


**Figure 1.** GPC profiles of SI diblock and $(SIS)_p$ multiblock copolymer samples.

The $SIS^-$ anion in the second batch was step-wisely copolymerized with I, S, and I monomers to give $SISISI^-$ anion; see the bottom part of Scheme 1. This $SISISI^-$ anion was further split into two batches and allowed to react with equimolar SI−Cl or bCMB. The crude products of these two batches were repeatedly fractionated from benzene/methanol mixtures to recover the $SISISI_2S$ heptablock and $SISISI_2SISIS$ undecablock samples.

**2.2. Characterization of Materials.** The block copolymer samples obtained as above and the precursors recovered after each step of polymerization were characterized with GPC (Co-8020 and DP8020, Tosoh) equipped with a refractive index (RI) monitor and a ultraviolet (UV) adsorption monitor (LS-8000 and UV-8020, Tosoh) connected in series. THF was the eluent, and previously synthesized/characterized monodisperse homopolyisoprenes[35,36] (hI) and commercially available monodisperse homopolystyrenes (hS; Tosoh TSK) were utilized as the elution standards as well as the reference materials for the RI/UV signal intensities. Figure 1 shows the GPC profiles of the copolymer samples. The S/I composition, seen as a ratio of the UV signal intensity (thin curves) to the RI signal intensity (thick curves), is indistinguishable for all samples.

The characterization was made for the GPC profiles with the standard method explained previously:[37] The weight-average molecular weight and the polydispersity index ($M_w/M_n$) of the first S block (common for all samples) were determined from the elution volume calibration utilizing the standard hS. For each multiblock copolymer, the molecular weight of the last-polymerized block was determined from the molecular weight of its ex-precursor in the prior step (e.g., the SIS ex-precursor for SISI shown in the middle part of Scheme 1) and the RI/UV signal intensities measured for the copolymer, the ex-precursor, and the hI/hS standards. Further details of this method were described elsewhere.[37] The polydispersity indices ($M_w/M_n$) of the copolymers were evaluated from the elution volume calibration utilizing the standard hI (because the I block was their major component). Table 1 summarizes the characteristics of the samples thus determined. For all samples, the polydispersity index was smaller than 1.06.

As seen in Table 1, the molecular weight $M_S$ of the end S block is the same ($10^{-3}M_S = 10.4$) for all copolymer samples because they were synthesized from the same batch of $S^-$ block anion. We should also note that $M_S$ is almost identical for all inner S blocks of the penta-, hepta-, and undecablock samples ($10^{-3}M_S = 21.6$ and 21.8) and this $M_S$ value is close to twice of $M_S$ of the end S block. Furthermore, $M_I$ is almost identical for all I blocks of the multiblock samples ($10^{-3}M_I = 36.8-40.6$) and this $M_I$ value is close to twice of $M_I$ for the SI diblock sample ($10^{-3}M_I = 20.3$).

**Table 1. Characteristics of Block Copolymer Samples[l]**

| $10^{-3}M$ | SI diblock | $SI_2S$ triblock | $SISI_2S$ pentablock | $SISI_2SIS$ heptablock | $SISISI_2S$ heptablock | $SISISI_2SISIS$ undecablock |
|---|---|---|---|---|---|---|
| first block (S) | 10.4[a] | 10.4[a] | 10.4[a] | 10.4[a] | 10.4[a] | 10.4[a] |
| second block (I) | 20.3[b] | 40.6[c,m] | 37.1[d] | 37.1[d] | 37.1[d] | 37.1[d] |
| third block (S) | | 10.4[a] | 21.6[e] | 21.6[e] | 21.6[e] | 21.6[e] |
| fourth block (I) | | | 38.7[f,m] | 36.8[g,m] | 38.0[h] | 38.0[h] |
| fifth block (S) | | | 10.4[a] | 21.6[e] | 21.8[i] | 21.8[i] |
| sixth block (I) | | | | 37.1[d] | 40.5[j,m] | 40.4[k,m] |
| seventh block (S) | | | | 10.4[a] | 10.4[a] | 21.8[i] |
| eighth block (I) | | | | | | 38.0[h] |
| ninth block (S) | | | | | | 21.6[e] |
| 10th block (I) | | | | | | 37.1[d] |
| 11th block (S) | | | | | | 10.4[a] |

[a] Identical to $M_{S1}$ shown in Scheme 1. [b] Identical to $M_{I1}$ shown in Scheme 1. [c] Identical to $2M_{I1}$ shown in Scheme 1. [d] Identical to $M_{I2}$ shown in Scheme 1. [e] Identical to $M_{S2}$ shown in Scheme 1. [f] Identical to $M_{I1} + M_{I3}$ shown in Scheme 1 ($M_{I3} = 18.4 \times 10^3$). [g] Identical to $2M_{I3}$ shown in Scheme 1. [h] Identical to $M_{I4}$ shown in Scheme 1. [i] Identical to $M_{S3}$ shown in Scheme 1. [j] Identical to $M_{I1}+M_{I5}$ shown in Scheme 1 ($M_{I5} = 20.2 \times 10^3$). [k] Identical to $2M_{I5}$ shown in Scheme 1. [l] The polydispersity index was smaller than 1.06 for all samples, and the $M$ values shown here are the values of the weight-average molecular weight. [m] $I_2$ block having a symmetrically once-inverted dipole.

This matching of the block molecular weights is visually confirmed for the almost indistinguishable GPC profiles of the two heptablock samples ($SISISI_2S$ and $SISI_2SIS$ in Figure 1) synthesized from different routes. The matching was successfully achieved because the volumes of the S and I monomers utilized in respective steps of polymerization and the volumes of the precursor solutions taken from the polymerizing batches were carefully measured with long ampules having fine grids.

The $SI_2S$ triblock sample was synthesized through the head-to-head coupling of the precursor $SI^-$ anion and was an exact dimer of SI. As for the *molecular weights* of the block sequence, the pentablock sample, two heptablock samples, and the undecablock sample, respectively, are equivalent to the dimer, trimer, and pentamer of $SI_2S$; see Table 1. Thus, we utilize the abbreviation $(SIS)_p$ with $p$ indicating the number of repeating SIS units; $p = 1$, 2, 3, and 5 for the tri-, penta-, hepta-, and undecablock copolymers. All these copolymers are symmetric with respect to the block sequence and have the same S blocks at the chain ends.

As for *the dipole arrangement*, our multiblock copolymers had no equivalence to the multimer of $SI_2S$. The $SI_2S$ triblock, $SISI_2$-SIS heptablock, and $SISISI_2SISIS$ undecablock samples, being synthesized through head-to-head coupling of respective precursor anions, were perfectly symmetric with respect to both of the dipole arrangement and block sequence; cf. Table 1. The center $I_2$ blocks of these samples have the symmetrically once-inverted dipoles, and the off-center I blocks have no inversion of dipole.

The $SISI_2S$ pentablock and $SISISI_2S$ heptablock samples were obtained through coupling of respective precursor anions with SI−Cl and had the dipole inversion only in one of the off-center I blocks. Since $M_I$ of the last-polymerized I block of these precursor anions ($M_{I3} = 18.4 \times 10^3$ and $M_{I5} = 20.2 \times 10^3$; cf. Scheme 1 and Table 1) was close to $M_I$ for SI−Cl ($M_{I1} = 20.3 \times 10^3$), the $I_2$ block of these samples had the dipoles almost symmetrically inverted at its the center.

Here, we should emphasize that the $SISISI_2S$ and $SISI_2SIS$ heptablock samples had almost indistinguishable molecular weights for the block sequences (cf. Figure 1 and Table 1) but different locations of the dipole-inverted $I_2$ block. This difference enabled us to dielectrically examine the bridge fraction for different portions of the heptablock chains, as explained later in more details.

**2.3. Measurements.** The systems subjected to rheological, dielectric, and small-angle X-ray scattering (SAXS) measurements were 40 wt % solutions of the SI diblock and the $(SIS)_p$ multiblock samples, the latter having the dipole inversion in particular I block-(s); cf. Table 1. The solvent was *n*-tetradecane (C14), a nonvolatile selective solvent dissolving the I blocks and precipitating the S blocks at room temperature or lower. In these solutions, the S blocks had a volume fraction of $v_S = 0.11$ and formed bcc spherical domains (as noted from the SAXS measurements at 20 °C). For comparison, the dielectric behavior was examined also for a 40 wt % C14 solution of the SIS precursor having no inversion of the dipole (cf. Scheme 1). These solutions were prepared by first dissolving prescribed masses of the copolymer sample and C14 in benzene to make homogeneous, dilute solutions (of copolymer concentration of ≅5 wt %) and then allowing benzene to thoroughly evaporate. The SI/C14 solution was a plastic fluid while the $(SIS)_p$/C14 solutions were elastic gels at room temperature.

For these solutions, dynamic linear viscoelastic measurements were made at 20 °C with a laboratory rheometer (ARES, Rheometrics). A parallel-plate fixture of a diameter = 8 mm was utilized. The storage and loss moduli, $G'$ and $G''$, were measured as functions of the angular frequency $\omega$ (in a range of $\omega/s^{-1} = 10^{-2}-10^2$). The amplitude of the oscillatory strain was kept small (=0.01) to ensure the linearity of the $G'$ and $G''$ data. For the $(SIS)_p$ systems, a constant rate extensional test was also made at 20 °C with an Extensional Viscosity Fixture (EVF; Rheometrics) mounted on ARES. Samples cut into rectangular sheets of length = 20 mm, width = 9−10 mm, and thickness = 0.3−0.4 mm were utilized.

For the SI/C14 and $(SIS)_p$/C14 systems charged in a dielectric cell composed of parallel electrodes and a guard electrode, dielectric measurements were conducted at 5 and 20 °C with an impedance analyzer/dielectric interface system (1260 and 1296, Solartron) and a capacitance bridge (1615A, QuadTech). The dielectric loss $\epsilon''$ was measured as a function of $\omega$ between $10^3$ and $10^7$ $s^{-1}$. The applied electric field was kept small (<1 V/mm) to ensure the linearity of the $\epsilon''$ data. The data at $T = 5$ and 20 °C obeyed the time−temperature superposition, confirming that the microdomain structure involving the glassy S domains did not change at those $T$. The data were reduced at 20 °C and compared with the rheological data at 20 °C.

SAXS measurements were made at 20 °C with a laboratory goniometer (RINT-2000, Rigaku) equipped in Professor Kanaya's laboratory in Institute for Chemical Research, Kyoto University. The wavelength of X-ray was $\lambda = 0.154$ nm (Cu Kα line). The samples were charged in a cell having a mica window, and the scattering intensity $I(q)$ was measured as a function of the magnitude of scattering vector $q = \{4\pi/\lambda\}\sin(\theta/2)$ with $\theta$ being the scattering angle. No desmearing correction was made for the $I(q)$ data.

## 3. Results and Discussion

**3.1. Linear Viscoelastic Behavior and Structure.** For the 40 wt % C14 solutions of the SI diblock and $(SIS)_p$ multiblock copolymers at 20 °C, Figure 2 shows plots of the storage and loss moduli, $G'$ (large symbols) and $G''$ (small symbols), against the angular frequency $\omega$. All these systems exhibit equilibrium elasticity characterized with the $G'$ plateau at low $\omega$ and much smaller values of $G''$, and the $G'$ data are nearly the same for

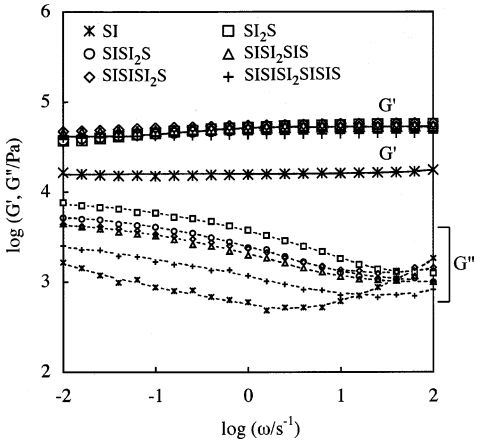


**Figure 2.** Storage and loss moduli, $G'$ (large symbols) and $G''$ (small symbols), obtained for the SI/C14 and $(SIS)_p$/C14 systems ($C_{copolymer}$ = 40 wt %) at 20 °C.

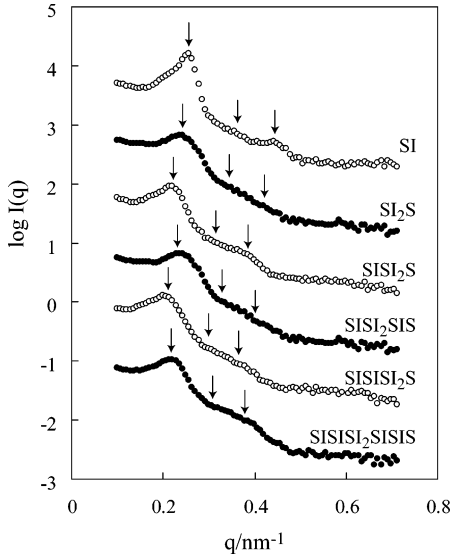


**Figure 3.** Plots of SAXS intensity $I(q)$ of SI/C14 and $(SIS)_p$/C14 systems ($C_{copolymer}$ = 40 wt %) at 20 °C against the wave vector $q$. The plots for respective systems are vertically shifted to avoid heavy overlapping of the data points.

all multiblock systems. The equilibrium modulus evaluated as the $G'$ value at the lowest $\omega$ is

$$G_e = 1.6 \times 10^4 \text{ Pa for SI/C14} \quad (1)$$

$$G_e = \{4.1 \pm 0.4\} \times 10^4 \text{ Pa for } (SIS)_p\text{/C14} \quad (p = 1, 2, 3, \text{and } 5) \quad (2)$$

The $G_e$ of the multiblock systems is larger than $G_e$ of the SI system only by a factor of ≅ 2.5, which indicates that the tail-type I blocks in the diblock system sustain a significant elasticity under the osmotic constraint for their conformation, as explained later in more details.

For these systems, plots of the SAXS intensity $I(q)$ against the scattering vector $q$ are shown in Figure 3. The plots for respective systems are vertically shifted to avoid heavy overlapping of the data points. For the SI diblock system, the first to third-order scattering peaks are observed at the scattering vectors satisfying a ratio, $q_1:q_2:q_3 = 1:\sqrt{2}:\sqrt{3}$; see arrows in the top part of Figure 3. This ratio suggests that the S blocks (minor component having the volume fraction $v_S = 0.11$ in the system) formed spherical domains arranged on a bcc lattice, which is

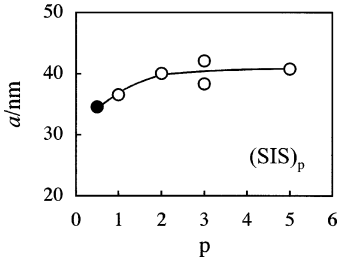


**Figure 4.** Cell-edge length of the bcc lattice of the S domains in $(SIS)_p$/C14 systems ($C_{copolymer}$ = 40 wt %) at 20 °C. The data for these systems (unfilled circles) are plotted against the number of repeating SIS unit, $p$. The two data points for $p = 3$ indicate the cell edge lengths obtained for two heptablock systems, $SISI_2SIS$ (lower point) and $SISISI_2S$ (upper point). For comparison, the data for 40 wt % SI/C14 system (filled circle) is plotted at $p = 0.5$.

in harmony with the structure in similar SI/C14 systems.[10,15] Similarly, the $(SIS)_p$ multiblock systems exhibit the first-order peak and higher order peaks/shoulders at $q_1:q_2:q_3 = 1:\sqrt{2}:\sqrt{3}$ (see arrows) and thus form bcc lattices, although these lattices are considerably distorted and not of high coherence, as noted from the broadness of the peaks/shoulders.

In Figure 4, the cell-edge length of the lattice in the $(SIS)_p$ multiblock systems evaluated from $q_1$ of the first-order scattering peak, $a = 2\sqrt{2}\pi/q_1$, is plotted against the repeating unit number, $p$; see unfilled circles. The filled circle indicates the cell-edge length for the SI diblock system (plotted at $p = 0.5$). This length increases moderately (by a factor of ≅ 15%) with increasing $p$ and approaches an asymptotic value of $a \cong 40$ nm at $p \geq 2$. For lamellar-forming $(SIS)_p$ multiblock systems, Wu and co-workers[7] observed a similar increase of the lamellar spacing and discussed this increase in terms of the $p$ dependence of the order−disorder transition point (specified by a product of the interaction parameter $\chi$ and the polymerization index $N$).

The SI diblock system contains no bridges connecting the S domains but exhibits the equilibrium elasticity under small strains (cf. Figure 2). This elasticity is sustained by the tail-type I blocks that osmotically stabilize the bcc lattice of the S domains[8,10,11] (cf. top part of Figure 3). In relation to this point, it is informative to compare the measured equilibrium modulus $G_e$ (eq 1) with the modulus expected for the simplest case in which each tail-type I block behaves as an *independent* entropic unit

$$G_{e,SI}^{\circ} = F\nu_I k_B T = 4.4 \times 10^4 \text{ Pa for SI} \quad (3)$$

Here, $\nu_I$ (=7.5 × $10^{18}$ $cm^{-3}$) is the number density of the I blocks in the I/C14 matrix phase in the SI system, $k_B$ is the Boltzmann constant, and $T$ is the absolute temperature. The front factor, $F = 1 + 2.5v_S + 14.1v_S^2$ (≅1.45),[38] represents the filler effect of the spherical, glassy S domains (having the volume fraction $v_S = 0.11$ in the system). The measured $G_e$ (eq 1) is considerably smaller than this $G_{e,SI}^{\circ}$ due to the osmotic constraint for the I block conformation: The I blocks are required to maintain the uniform concentration distribution in the I/C14 matrix phase. Since the I blocks are tethered on the S domains, this requirement forces neighboring I blocks to have correlated conformations. The lattice is formed in order to minimize the loss of conformational entropy under this constraint,[10,11] and $G_e$ reflects the entropy loss on deformation of the lattice. All blocks do not behave as the independent entropic units because of the conformational correlation, and an effective number density of independent unit is smaller than $\nu_I$ to give $G_e < G_{e,SI}^{\circ}$.[11]

The multiblock systems exhibited the gel-like elasticity (even under large deformation, as shown later). It is also interesting to examine their $G_e$ data (eq 2). We note that the measured $G_e$ is larger than the modulus for an ideal case in which each I block as a whole behaves as an independently stress-sustaining unit, $G_{e,(SIS)p}^{\circ} = F\nu_I k_B T \cong 2.2 \times 10^4$ Pa ($\nu_I \cong 3.7 \times 10^{18}$ cm$^{-3}$ for the $(SIS)_p$ copolymers). Because of this difference, we tend to consider that the I/C14 matrix in the multiblock systems is equivalent to a homo-polyisoprene (hI) solution but all entanglements in this solution are effectively trapped in the multiblock systems. For this simplest case, the equilibrium modulus is expected to be[39]

$$G_{e,ent}^{\circ} = FG_{N,bulk}\varphi_I^2 \cong 4.8 \times 10^4 \text{ Pa for } (SIS)_p \qquad (4)$$

Here, $G_{N,bulk}$ ($\cong 4.6 \times 10^5$ Pa at 20 °C)[40] is the entanglement plateau modulus of bulk hI, $\varphi_I$ (=0.27) is the volume fraction of the I blocks in the I/C14 matrix phase, and the factor $F$ ($\cong$1.45) represents the filler effect due to the S domains. The $G_e$ data of the multiblock systems (eq 2) is close to this $G_{e,ent}^{\circ}$. This result can be related to the entanglement molecular weight for the I block with $\varphi_I = 0.27$,[39]

$$M_e = M_{e,bulk}/\varphi_I = 19 \times 10^3 \qquad (5)$$

where $M_{e,bulk} = 5 \times 10^3$ is the entanglement molecular weight for bulk hI.[40] The I blocks of the multiblock copolymers have the molecular weight close to $2M_e$ and they form light entanglements, and the entanglements formed by the bridge-type I blocks connecting the S domains are trapped in the copolymer systems.

In relation to this point, we should emphasize that the multiblock systems unequivocally include the dangling loop-type I block in addition to the bridge-type I block, the former being entangled in the dynamic sense (because it has $M \cong 2M_e$) but forming no permanently trapped entanglement. These dangling loops should also contribute to the equilibrium elasticity with the mechanism similar to that for the tail-type I blocks of SI (osmotically induced correlation of the block conformation).[8] Thus, the close agreement of the $G_e$ data of multiblock systems (eq 2) and $G_{e,ent}^{\circ}$ (eq 4) is not indicative of the *complete* validity of the simplest molecular picture (the similarity with the entangled hI solution). Instead, the bridge elasticity would be reduced a little while the loop elasticity should be enhanced in the presence of the osmotic constraint, as fully discussed in the previous papers.[8] Keeping this feature in mind, we examine the dielectric behavior of the diblock and multiblock systems in the next section.

**3.2. Dielectric Behavior. 3.2.1. Overview.** For the SI diblock and $(SIS)_p$ multiblock copolymers dissolved in *n*-tetradecane ($C_{copoymer}$ = 40 wt %), the angular frequency ($\omega$) dependence of the dielectric loss $\epsilon''$ reduced at 20 °C is shown in the top panel of Figure 5; see filled and unfilled symbols. The solid curves are a guide for eye. For comparison, the data for the SIS prepolymer without dipole inversion (cf. Scheme 1) are shown with the plus symbol. Since the glassy S domains are dielectrically inert, the observed dielectric relaxation is attributed to the large-scale motion of the I blocks having the type-A dipole, as explained later in more details. (The local, segmental relaxation of the I blocks occurs at high frequencies out of our experimental window.)

In general, the microscopic polarization **P** of the I block is given by a vectorial sum of its dipoles, and the dielectric relaxation reflects the thermal fluctuation of **P**.[10,29] As shown in Figure 6a, the I block of the SI copolymer has the tail-type

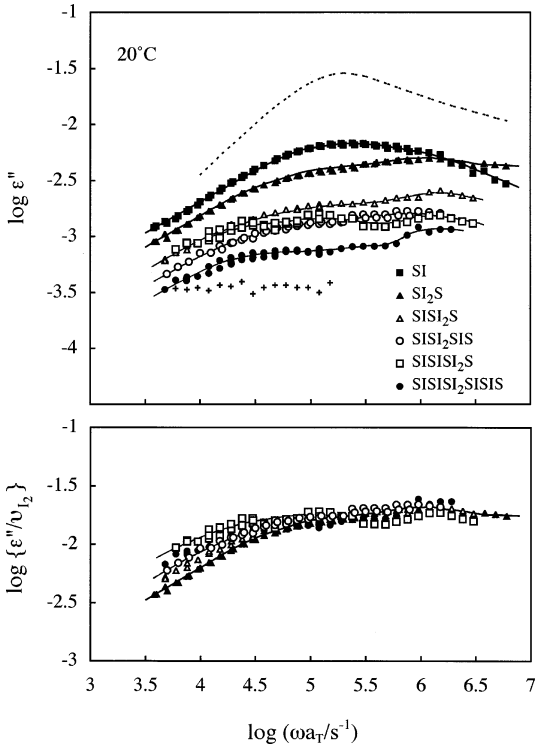


**Figure 5.** Top panel: Plots of dielectric loss $\epsilon''$ of SI/C14 and $(SIS)_p$/C14 systems ($C_{copolymer}$ = 40 wt %) against the angular frequency $\omega$; see filled and unfilled symbols. The solid curves are a guide for eye. For comparison, the data for the SIS prepolymer without dipole inversion are shown with the plus symbol. The dotted curve indicates the $\epsilon''$ data of a dipole-inverted homo-polyisoprene (hI; $M = 47.7 \times 10^3$). This curve is shifted along the $\omega$ axis to match its peak frequency with that for the SI/C14 system. Bottom panel: Plots of the normalized dielectric loss $\epsilon''/\upsilon_{I2}$ of the $(SIS)_p$/C14 systems ($\upsilon_{I2}$ = volume fraction of the dipole-inverted $I_2$ block in the systems).

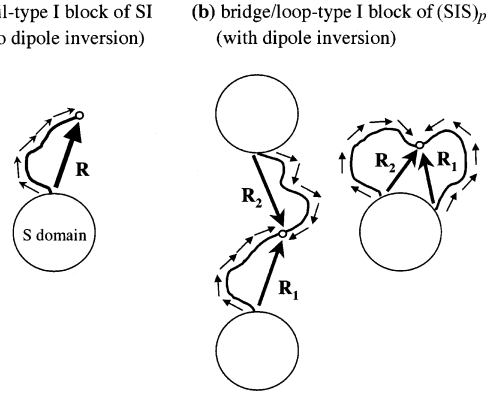


**Figure 6.** Schematic illustration of the tail-type I block of SI and the bridge- and loop-type $I_2$ blocks of $(SIS)_p$. Thin arrows indicate the type-A dipoles of these blocks. The tail has noninverted dipoles, while the bridge and loop have symmetrically once-inverted dipoles.

conformation and its type-A dipoles are arranged along the chain backbone without inversion. Thus, **P** of this I block is proportional to the end-to-end vector **R**, and the fluctuation of **R** due to the motion of the free end of the tail results in the dielectric relaxation of the SI system.

In contrast, the I block of the $(SIS)_p$ multiblock copolymers has the bridge/loop-type conformation and its two ends are *immobilized* at the surface of glassy S domains; cf. Figure 6b. Thus, no slow dielectric relaxation is activated by the motion of such I block if it has no inversion of the dipole, which is the case for the SIS prepolymer system: The $\epsilon''$ of this system, shown with the plus symbol in the top panel of Figure 5, has

values at the level of background noise ($\epsilon'' \sim 10^{-3.5}$) and exhibits no dispersion. However, if the I block has a symmetrical inversion of its type-A dipoles, the polarization **P** is proportional to a sum of two end-to-center vectors $\mathbf{R}_1$ and $\mathbf{R}_2$ (cf. Figure 6b) and thus the motion of the midpoint of the I block activates the dielectric relaxation.[8,10,25] The dielectric relaxation seen for the dipole-inverted $(SIS)_p$ systems (filled/unfilled symbols in Figure 5) is exclusively attributable to this midpoint motion, as discussed later in more details. In relation to this fact, we note that the dipole-inverted $I_2$ block gives a clear dielectric signal larger than the background noise even if this block has just a small volume fraction $v_{I2}$ in the system; compare the signals from the dipole-inverted $SISISI_2SISIS$ undecablock system ($v_{I2} = 0.05$; filled circle) and the SIS system without dipole inversion ($v_I = 0.20$; plus symbol at the background noise level).

**3.2.2. Mode Distribution of SI.** Here, we examine the dielectric mode distribution of the SI system observed through the $\omega$ dependence of the $\epsilon''$ data. For this purpose, we first compare the $\epsilon''$ data of the SI system with the data previously obtained for a bulk system of linear homopolyisoprene (hI)[30] having symmetrically once-inverted dipoles. In the top panel of Figure 5, the dotted curve indicates the $\epsilon''$ data of this hI having the molecular weight ($=47.7 \times 10^3$) close to that of the dipole-inverted $I_2$ block of our $(SIS)_p$ copolymers. The hI data are arbitrarily shifted along the $\omega$ axis to match their $\epsilon''$-peak frequency with that for the SI system,

$$\omega_{peak}(SI) \cong 2 \times 10^5\ s^{-1} \tag{6}$$

Clearly, hI has a narrow distribution of the dielectric modes, as noted from its sharp $\epsilon''$-peak that is immediately followed by the low-$\omega$ terminal tail characterized by a proportionality, $\epsilon'' \propto \omega$. This mode distribution is insensitive to the entanglement and hardly changes on moderate dilution of hI to a volume fraction of $v_I = 0.3$ (and becomes a little narrower on further dilution).[41] The mode distribution of the SI system (filled squares) is much broader, in particular in the low-$\omega$ side (long time side) where the $\epsilon''$ data exhibit no terminal tail but less $\omega$-dependent power-law behavior, $\epsilon'' \propto \omega^\beta$ with $\beta \cong 0.6$. This lack of the terminal tail, noted also for similar SI micellar systems,[8,10] is indicative of significant broadening of the dielectric mode of SI.

The broad dielectric mode distribution can, in principle, result from several different factors such as the entanglement of the tail-type I blocks, the spatial confinement (steric repulsion) for the I blocks due to the glassy S domains,[42−44] the relaxation of the coherent interfaces of the grains of SI copolymers,[45] and the osmotic constraint for the I blocks.[8,10,11,25,42] However, the entanglement is irrelevant to the I blocks of our SI having a rather low $M_I$ ($=20.3 \times 10^3$; Table 1): The entanglement effect becomes significant only for $M_I \geq 2M_e$ (with $M_e = 19 \times 10^3$; eq 5). The spatial confinement due to the glassy S domain (on which the I block is tethered) gives just a secondary effect on the block motion,[42,43] in particular in our system where the S domains have a small volume fraction ($v_S = 0.11$) and the I blocks are not entangled. This confinement is not responsible for the mode broadening seen for our SI system. The relaxation of the coherent interface is much slower than the relaxation of individual I blocks to give a bimodal shape of the $\epsilon''$ curve. Thus, this relaxation does not seem to be responsible for the broadening of the unimodal $\epsilon''$ curve of our SI (although the interface relaxation may occur at low frequencies not covered in our experiments).

Thus, the mode broadening seen for our SI system can be attributable to the last factor, the osmotic constraint for the I block:[8,10,11,25,42] The I blocks are osmotically required to maintain a uniform concentration distribution in the I/C14 matrix phase. Since the concentration and conformation of the *tethered* I blocks are strongly coupled, this requirement forces the neighboring I blocks to have correlated conformations. This correlation, leading to the formation of the lattice of the S domains and providing the system with the equilibrium elasticity, results in a cooperativity of the large-scale motion of the I blocks which naturally broadens the dielectric mode distribution.

**3.2.3. Mode Distribution of $(SIS)_p$.** Here, we examine the dielectric mode distribution for the series of $(SIS)_p$ multiblock copolymers. As seen in Figure 5, these copolymers exhibit double-peaked $\epsilon''$ curves and have a broad and *bimodal* mode distribution. One may suspect that this distribution could result from the spatial confinement due to the glassy S domains[42−44] and/or the relaxation of the coherent interface of the copolymer grains.[45] However, the spatial confinement does not seem to have a large effect in our copolymer systems having small $v_S$ (=0.11). In addition, if this confinement has a significant effect, it would broaden the unimodal mode distribution but lead to no bimodal distribution, as judged from the data for $(SI)_4$ star block copolymers.[44] The interface relaxation is much slower than the relaxation of the I blocks, thereby giving a bimodal mode distribution.[45] However, our $(SIS)_p$ copolymers exhibit the bimodal distribution at frequencies where the I blocks in the SI system relax (cf. Figure 5). These frequencies appear to be too high to be related to the interface relaxation. Furthermore, the interface relaxation should occur irrespective of the inversion of the dipoles of the I blocks, but no significant relaxation is detected for the SIS prepolymer having no inversion; see the plus symbols in the top panel of Figure 5. Thus, the broad and bimodal mode distribution seen for the $(SIS)_p$ copolymers can be related to the midpoint motion of the dipole-inverted $I_2$ blocks under the osmotic constraint. These blocks are lightly entangled and thus their relaxation is a little affected by the entanglement, as explained later in the analysis of the bridge fraction.

For a detailed examination of this mode distribution, the $\epsilon''$ data of the $(SIS)_p$ copolymers are normalized by the volume fraction of the dipole-inverted $I_2$ block in the system, $v_{I2}$, and plotted against $\omega$ in the bottom panel of Figure 5. Since the I blocks in the systems have either bridge- or loop-type conformation and both of the bridge and loop contribute to $\epsilon''$, the normalized $\epsilon''/v_{I2}$ data can be expressed as

$$\epsilon''(\omega)/v_{I2} = \phi_{bridge}\tilde{\epsilon}_{bridge}''(\omega) + \phi_{loop}\tilde{\epsilon}_{loop}''(\omega) \tag{7}$$

Here, $\phi_{bridge}$ and $\phi_{loop}$ ($=1 - \phi_{bridge}$) are the number fractions of the bridge- and loop-type $I_2$ blocks, respectively, and $\tilde{\epsilon}_{bridge}''(\omega)$ and $\tilde{\epsilon}_{loop}''(\omega)$ indicate the dielectric loss of the bridge- and loop-type $I_2$ blocks normalized to unit volume fraction.

Since the I block molecular weight and concentration are indistinguishable for all multiblock systems, $\tilde{\epsilon}_{bridge}''(\omega)$ and $\tilde{\epsilon}_{loop}''(\omega)$ should have common values in these systems. Then, the normalized $\epsilon''/v_{I2}$ data should be the same for all systems irrespective of the $\phi_{bridge}$ value *if* $\tilde{\epsilon}_{bridge}''(\omega) = \tilde{\epsilon}_{loop}''(\omega)$; see eq 7. However, differences of the $\epsilon''/v_{I2}$ data are clearly noted in the bottom panel of Figure 5, though the differences are not very large (within a factor of 2). This result leads us to conclude that the dipole-inverted bridge and loop give different dielectric responses, i.e., $\tilde{\epsilon}_{bridge}''(\omega) \neq \tilde{\epsilon}_{loop}''(\omega)$. Furthermore, we may conclude, with no ambiguity, that $\phi_{bridge}$ changes with the block location as noted from the difference of the $\epsilon''/v_{I2}$ data of the $SISI_2SIS$ and $SISISI_2S$ heptablock copolymers and that $\phi_{bridge}$ also changes with the total block number as noted from the

difference seen for the $SI_2S$ triblock, $SISI_2SIS$ heptablock, and $SISISI_2SISIS$ undecablock copolymers all having the dipole-inverted $I_2$ block at the chain center. (Note that the $\epsilon''/v_{I2}$ data should be the same for all $(SIS)_p$ systems if $\phi_{bridge}$ is the same for all systems; cf. eq 7.)

The above results suggest that $\phi_{bridge}$ can be estimated from the dielectric data. For convenience of this estimation, we first compare the dielectric mode distribution of the $SI_2S$ and SI systems (filled triangle and square in the top panel of Figure 5). The mode distribution of the $SI_2S$ system is broader than that of the SI system and slightly bimodal. Two broad peaks of the $\epsilon''$ curve of $SI_2S$ are seen at

$$\omega_{slow-peak}(SI_2S) \cong 1 \times 10^5\ s^{-1} \quad \text{and} \quad \omega_{fast-peak}(SI_2S) \cong 2 \times 10^6\ s^{-1} \quad (8)$$

(A similar, broadly double-peaked $\epsilon''$ curve is noted for a previously examined $SI_2S$ system at a high concentration, 50 wt %.[8])

The SI system contains only single species, the tail-type I block, while the $SI_2S$ system includes two species, the bridge- and loop-type $I_2$ blocks. The effect of the osmotic constraint on the midpoint motion should be different for the bridge and loop, as suggested from the difference between $\tilde{\epsilon}_{bridge}''(\omega)$ and $\tilde{\epsilon}_{loop}''(\omega)$ explained above. Furthermore, at low $\omega < \omega_{slow-peak}$, the $SI_2S$ system exhibits the nonterminal power-law behavior very similar to that of the tail-type I block of SI, $\epsilon'' \propto \omega^{\beta}$ with $\beta \cong 0.6$. These results tempt us to assign the slow relaxation characterized with this power-law behavior to one species (loop- or bridge-type $I_2$ block) being affected by the osmotic constraint in a way similar to that for the tail-type I block. Then, the fast relaxation characterized with the peak at $\omega_{fast-peak}$ is attributed to the other species.

The double-peaked $\epsilon''$ curve is more clearly noted for the penta-, hepta-, and undecablock copolymers; cf. Figure 5. The peak frequencies seen for these copolymers are close to those for the $SI_2S$ copolymer (eq 8), and the nonterminal power-law behavior at low $\omega$ ($\epsilon'' \propto \omega^{\beta}$ with $\beta \cong 0.6$) is commonly seen for all of these copolymers. These results again tempt us to assign the slow relaxation of the penta-, hepta-, and undecablock copolymers to one species (loop or bridge) and the fast relaxation to the other species.

**3.3. Dielectric Estimation of Bridge Fraction.** Considering the dielectric feature of the $(SIS)_p$ multiblock copolymers seen in Figure 5, we here attempt to dielectrically estimate the bridge fraction $\phi_{bridge}$ for the $I_2$ block of these copolymers. For this estimation, Watanabe et al.[8,15,25] made the following argument. For the I blocks having fixed ends, the concentration profile is strongly coupled with the block conformation and thus the osmotic requirement of maintaining the uniform profile forces the neighboring blocks to move in a highly cooperative way. The loop and bridge are composed of two half-fragments, and the tension and friction of each fragment are the same as those for the tail. For the loop, the two fragments always pull the midpoint to the same direction to feel the same osmotic penalty for their motion (cf. Figure 6). Since this penalty is similar to that for the tail, the midpoint fluctuation of the dangling loop would be similar to the end fluctuation of the tail, which suggests a similarity of the slow dielectric responses of the tail and loop. In contrast, for the bridge, the two fragments pull the midpoint in the opposite direction (cf. Figure 6), and an increase of the osmotic penalty for one fragment tends to be cancelled by a decrease of the penalty for the other: For example, a highly compressed, unfavorable conformation of one bridge fragment releases the compression for the other. Thus, the midpoint fluctuation of the bridge appears to be associated with a smaller penalty compared to the fluctuation of the loop, which suggests that dielectric relaxation is faster for the bridge than for the loop and the dielectric intensity at low $\omega$ is smaller for the former.

The above hypothesis of the dielectric similarity between the loop and tail is consistent with an experimental result that the difference between the $\epsilon''$ data of SI and $SI_2S$ systems almost vanishes at low concentrations where the bridge should be stretched/destabilized and the loop should become the dominant component in the $SI_2S$ system.[8] The hypothesis is also consistent with the other result that the $\epsilon''$ data of $SI/SI_2S$ blend hardly change with the SI weight fraction $w_{SI}$ in a range of $w_{SI} \leq 0.3$:[26] The hypothesis suggests that the blending of SI is equivalent to an addition of loops to the $SI_2S$ system and the reequilibration of $SI_2S$ conformation can keep the same bridge/(loop+tail) population distribution to give the same $\epsilon''$ for relatively small $w_{SI}$ values.

Despite these experimental supports, the hypothesis has not been justified from the first principle of the dynamics of osmotically constrained block chains (which itself has not been fully established). In addition, the hypothesis fails when the loop forms dense knots (densely trapped entanglements) with the other loops/bridges.[8] However, no $\phi_{bridge}$ data have been obtained from experiments based on so-called absolute methods (e.g., SANS),[20] as explained earlier. Thus, in this study, we adopt the hypothesis of the similarity between the loop and tail to dielectrically estimate $\phi_{bridge}$ for the $I_2$ blocks of the $(SIS)_p$ multiblock copolymers. (The I blocks in our $(SIS)_p$ systems form light knots but no dense knots, as discussed earlier for Figure 2.) With this hypothesis, the fast and slow dielectric relaxation processes of these copolymers seen in Figure 5 are assigned as the processes for the bridge- and loop-type $I_2$ blocks, respectively.

The $\epsilon''$ data of the multiblock copolymers are unequivocally cast in the form of eq 7. The hypothesis of the similarity between the loop and tail suggests that the dielectric response of the loop normalized to unit volume fraction, $\tilde{\epsilon}_{loop}''(\omega)$ appearing in eq 7, is replaced by the normalized response of the tail, $\tilde{\epsilon}_{tail}''(\omega\Lambda)$, the latter being evaluated from the $\epsilon''$ data and the block number density of the SI system. Here, we have introduced a factor $\Lambda$ ($\geq 1$) not considered in the previous analysis.[8,15,25,26] This factor accounts for a small difference of the relaxation times of the tail and loop due to the transient (nontrapped) entanglement for the latter. (Our loop has $M \cong 2M_e$ ($=19 \times 10^3$; cf. eq 5) and forms light entanglements while our tail has $M \cong M_e$ and is in the nonentangled state.) Utilizing the $\epsilon''$-peak frequencies $\omega_{peak}(SI)$ and $\omega_{slow-peak}(SI_2S)$ (eqs 6 and 8), the latter being assigned to the loop in the $SI_2S$ system according to our hypothesis, the $\Lambda$ factor is estimated to be

$$\Lambda = \frac{\omega_{peak}(SI)}{\omega_{slow-peak}(SI_2S)} \cong 2 \quad (9)$$

With the above replacement, eq 7 is rewritten in a form that enables us to estimate the bridge and loop fractions, $\phi_{bridge}$ and $\phi_{loop}$ for $(SIS)_p$:

$$\epsilon_{(SIS)p}''(\omega) = v_{I_2}^{[(SIS)_p]}\phi_{bridge}\tilde{\epsilon}_{bridge}''(\omega) + \left\{\frac{v_{I_2}^{[(SIS)_p]}}{v_I^{[SI]}}\right\}\phi_{loop}\,\epsilon_{SI}''(\omega\Lambda) \rightarrow \left\{\frac{v_{I_2}^{[(SIS)_p]}}{v_I^{[SI]}}\right\}\phi_{loop}\,\epsilon_{SI}''(\omega\Lambda) \quad \text{at low } \omega \quad (10)$$

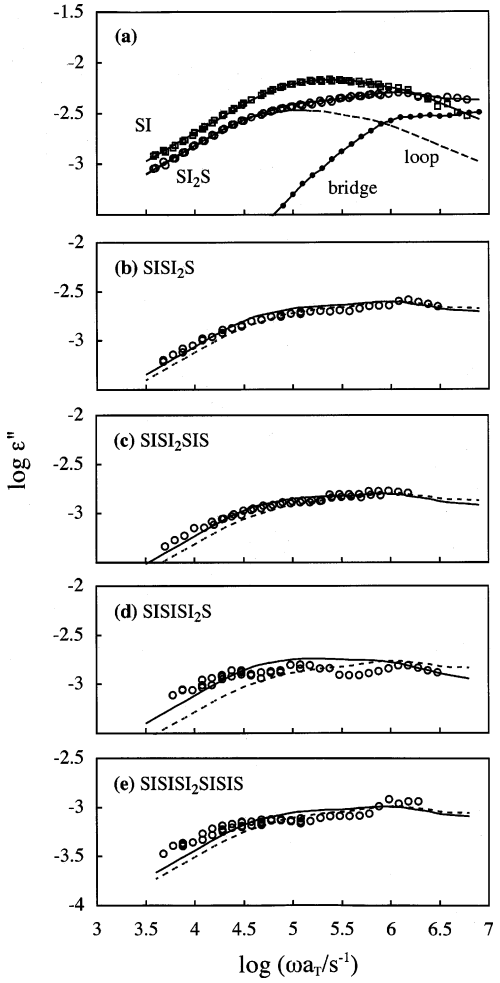


**Figure 7.** Fit of the $\epsilon''$ data of the $(SIS)_p$/C14 systems (circles) with eq 10 (solid curves). In parts b-e, dotted curves indicate the $\epsilon''$ data for the $SI_2S$ system just corrected for the content of the dipole-inverted $I_2$ block. For further details, see text.

Here, $v_{I_2}^{[(SIS)_p]}$ represents the known volume fraction of the dipole-inverted $I_2$ block in the multiblock systems, $v_I^{[SI]}$ is the I volume fraction in the SI system, and $\tilde{\epsilon}_{bridge}''(\omega)$ is the dielectric loss of the bridge reduced to unit volume fraction.

The relaxation should complete and the terminal tail ($\epsilon'' \propto \omega$) should emerge in a range of $\omega$ where the midpoint of the $I_2$ block fluctuates over a large length scale comparable to the block size. However, no terminal tail is observed in our experimental window (Figure 5), indicating that the measured $\epsilon''$ reflects the midpoint fluctuation over a relatively *short* length scale (as compared to the block size). Some loops in the $(SIS)_p$ systems should have formed light knots, but the effect of the light knots on the midpoint fluctuation over this short scale would be similar to the effect of the transient entanglements.[8,25] Thus, $\phi_{loop}$ estimated from the $\epsilon''$ data with the aid of eq 10 should be the *total* fraction of dangling (unknotted) loops and lightly knotted loops in the system.

Utilizing the $\epsilon_{SI}''(\omega\Lambda)$ data (with $\Lambda = 2$; eq 9), we fitted the $\epsilon_{SI_2S}''(\omega)$ data of the $SI_2S$ system with eq 10. The results are shown in Figure 7a. The dashed curve indicates the $\{v_{I_2}^{[SI_2S]}/v_I^{[SI]}\}\epsilon_{SI}''(\omega\Lambda)$ data multiplied by a factor of $\phi_{loop} = 0.50$. This curve is in close agreement with the $\epsilon_{SI_2S}''(\omega)$ data (circles) at $\omega < 1 \times 10^5$ s$^{-1}$, suggesting that $\phi_{bridge} = 1 - \phi_{loop} = 0.50$ is a good estimate for the bridge-type $I_2$ blocks in the $SI_2S$ system. We also made the fitting without the frequency correction for the loop (i.e., for $\Lambda = 1$) to obtain an estimate, $\phi_{loop} \cong 0.60$ ($\phi_{bridge} \cong 0.40$), although the quality of this fitting was a little worse than that for $\Lambda = 2$. Thus, the uncertainty of the estimated $\phi_{loop}$ value due to the frequency correction is about ±10% , and the estimate of $\phi_{bridge}$ ($=1 - \phi_{loop}$) includes the corresponding uncertainty.

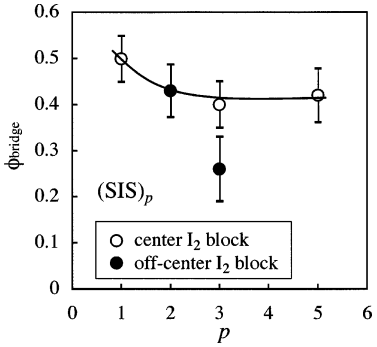


**Figure 8.** Changes of the dielectrically estimated bridge fraction $\phi_{bridge}$ of the dipole-inverted $I_2$ block of $(SIS)_p$ copolymers with the number of repeating SIS unit, $p$. Unfilled and filled circles indicate $\phi_{bridge}$ estimated for the center and off-center $I_2$ blocks, respectively. The error bar corresponds to ±10% uncertainty of $\phi_{loop}$ ( $= 1 - \phi_{bridge}$).

The dielectric response of the bridge in the $SI_2S$ system, $v_{I_2}^{[SI_2S]}\phi_{bridge}\tilde{\epsilon}_{bridge}''(\omega)$ obtained by subtracting the $\{v_{I_2}^{[SI_2S]}/v_I^{[SI]}\}\phi_{loop}\epsilon_{SI}''(\omega\Lambda)$ data from the $\epsilon_{SI_2S}''(\omega)$ data (cf. eq 10), is shown with the small filled circles in Figure 7a. Dividing this $v_{I_2}^{[SI_2S]}\phi_{bridge}\tilde{\epsilon}_{bridge}''(\omega)$ by the known value of $v_{I_2}^{[SI_2S]}$ and the $\phi_{bridge}$ estimate (=0.50), we evaluated the dielectric response of the bridge normalized to unit volume, $\tilde{\epsilon}_{bridge}''(\omega)$. We utilized this $\tilde{\epsilon}_{bridge}''(\omega)$ and the $\epsilon_{SI}''(\omega\Lambda)$ data (with $\Lambda = 2$) in eq 10 to fit the $\epsilon''$ data for the penta-, hepta-, and undecablock systems. The results are shown with the solid curves in Figure 7b−e. For appropriate estimates of the $\phi_{bridge}$ value shown later in Figure 8, the fitted curves agree with the data within the scatter of the data. In relation to this result, we should note that the data for the $SI_2S$ system just corrected for the content of the $I_2$ block, $\{v_{I_2}^{[(SIS)p]}/v_{I_2}^{[SI_2S]}\}\epsilon_{SI_2S}''(\omega)$ shown with the dotted curves, do not agree with the data in Figure 7b−e, in particular with the data for the $SISISI_2S$ heptablock system shown in Figure 7d. This result indicates that $\phi_{bridge}$ of the $I_2$ block changes with the location of this block in the copolymer backbone as well as with the total block number in the copolymer, as already explained for the bottom panel of Figure 5.

In Figure 8, the bridge fraction $\phi_{bridge}$ estimated from the fitting (Figure 7) is plotted against the repeating unit number $p$ of the $(SIS)_p$ copolymers. The error bar for $\phi_{bridge}$ corresponds to the ±10% uncertainty of $\phi_{loop}$ ($=1 - \phi_{bridge}$) explained earlier. The estimate of $\phi_{bridge}$ was obtained on the basis of the hypothesis of the similarity of the loop and tail and is to be regarded as a rough estimate. Nevertheless, Figure 8 demonstrates characteristic behavior of $\phi_{bridge}$ that deserves discussion: For the $I_2$ block located at the center of the multiblock chain, $\phi_{bridge}$ decreases slightly with increasing $p$ from 1 to 3 (from triblock to heptablock) and tends to level-off on a further increase of $p$ to 5 (to undecablock); see unfilled circles. We also note that $\phi_{bridge}$ for $p = 3$ is larger for the center $I_2$ block than for the off-center $I_2$ block.

The moderate decrease of $\phi_{bridge}$ for the center $I_2$ block on the increase of $p$ may partly reflect a moderate increase of the size $a$ of the lattice of the S domains (Figure 4): The bridge is stretched/destabilized at larger $a$ to decrease its $\phi_{bridge}$.[8] Thus, the decrease of $\phi_{bridge}$ and increase of $a$ may be commonly regarded as a transient effect due to the finite length of the copolymer chain. (Note that the $a$ and $\phi_{bridge}$ values become independent of $p$ for sufficiently large $p$). The difference of

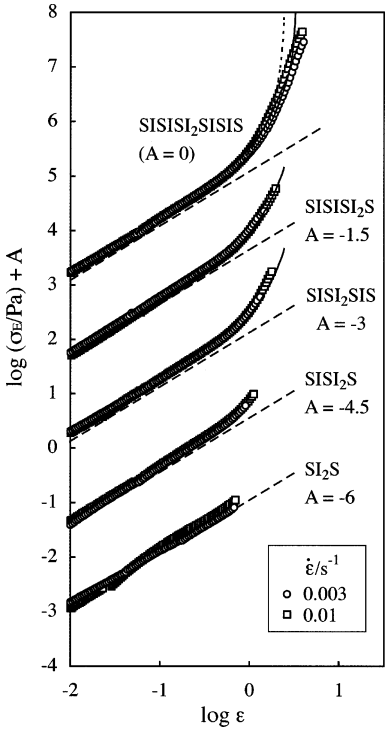


**Figure 9.** Dependence of the extensional stress $\sigma_E$ of the $(SIS)_p$/C14 systems on the Hencky strain $\epsilon$. The $\sigma_E$ data for respective systems are vertically shifted by factors $A$ as indicated to avoid heavy overlapping of the data points. The dashed lines indicate the linear elastic behavior expected from the equilibrium shear modulus. The solid and dotted curves indicate the stress calculated from the Edwards−Vilgis model. For further details, see text.

$\phi_{bridge}$ seen for the two heptablocks ($p = 3$) seems to be related to an effect of the S blocks at the end of the $(SIS)_p$ copolymers. Since the end S block is shorter than the inner S block (cf. Table 1), the packing in the S domain would be easier for the former. Then, the end S block of a given heptablock chain might tend to coexist in the same domain with the inner S block of this chain so as to reduce the thermodynamic penalty of the packing of the inner S block. If this is the case, the loop formation is enhanced for the off-center $I_2$ block, as observed. At this moment, no SCF calculation distinguishing the conformation of the center and off-center blocks of the sphere-forming multiblock copolymers is available. A further study is desired for this problem.

**3.4. Overview of Nonlinear Extensional Behavior.** The constant-rate extensional test was made for the $(SIS)_p$ multiblock systems at 20 °C. In Figure 9, the extensional stress $\sigma_E$ measured up to the rupture point is plotted against the Hencky strain $\epsilon$ ($= \dot{\epsilon}t$ with $\dot{\epsilon}$ being the Hencky strain rate). The $\sigma_E$ data of these systems were almost indistinguishable up to respective rupture points. Thus, the data for respective systems are vertically shifted by factors $A$ as indicated in order to avoid heavy overlapping of the plots. The $\sigma_E$ data obtained at two rates, $\dot{\epsilon} = 0.003$ and 0.01 $s^{-1}$, agree with each other, suggesting that the molecular relaxation process of the I blocks was completed in the time scale of the extensional test and hardly contributed to the $\sigma_E$ data. (Note that the $\dot{\epsilon}$ values utilized in the test were much smaller than the relaxation frequencies dielectrically observed in Figure 5).

In Figure 9, the dashed lines indicate the linear elastic extensional behavior expected from the equilibrium shear modulus $G_e$ (summarized in eq 2),

$$\sigma_E = 3G_e\epsilon \tag{11}$$

For all multiblock systems, this linear behavior is observed at $\epsilon < 0.7$ (at the stretch ratio $\lambda = \exp(\epsilon) < 2$). The $SI_2S$ system exhibits the rupture at $\epsilon \cong 0.8$ ($\lambda \cong 2.2$) while the rupture of the longer $(SIS)_p$ copolymers with $p \geq 2$ occurs at larger $\epsilon$ after significant strain-hardening. Clearly, the mechanical toughness is enhanced with increasing $p$. In particular, the $SISISI_2SISIS$ undecablock sample behaves as a tough gel characterized with the maximum strain $\epsilon_{max}$ and the maximum stretch ratio $\lambda_{max}$ attainable before the rupture,

$$\epsilon_{max} = 3.4 \quad \text{and} \quad \lambda_{max} = 30 \text{ for undecablock copolymer} \tag{12}$$

Since the glassy, discrete S domains (having the Young modulus $\cong 4 \times 10^9$ Pa at 20 °C) should deform only a little at the stress level seen in Figure 9 ($\sigma_E \leq 4 \times 10^7$ Pa), the I blocks in the undecablock system bear the net strain/stretch specified by eq 12. Usual cross-linked rubbers exhibit the rupture at smaller strain/stretch. An exception is the rubbers having the super-coiled conformation in their stands[46,47] (that bear the stretch up to $\lambda_{max} \cong 30$), but the I blocks in the $(SIS)_p$ systems *at rest* do not seem to have this conformation. Furthermore, the $(SIS)_p$ systems exhibit the hardening before the rupture, which is qualitatively different from the softening (weakening of $\lambda$ dependence of $\sigma_E$) seen for the super-coiled rubbers.[46,47]

The enhancement of the toughness on an increase of the block number is noted also for lamella-forming $(SI)_p$-type multiblock copolymers in bulk.[16] However, these lamellar copolymers exhibit the yielding/softening followed by the pseudo-plastic behavior[16,17] which corresponds to the fragmentation of the lamellar S domains. In contrast, our $(SIS)_p$ copolymers having spherical S domains exhibit only hardening before the rupture. For such $(SIS)_p$ copolymers, the rupture seems to occur through the pullout of the S blocks from the glassy S domains. Propagation of this chain pullout in the systems would be suppressed for larger $p$ (because more blocks are to be pulled out for larger $p$), which possibly results in the enhancement of the toughness seen in Figure 9. The hardening appears to reflect the tension of the bridge-type I blocks that are stretched to provide the system with the toughness until the rupture occurs.

This hardening behavior of the $(SIS)_p$ systems (Figure 9) is *qualitatively* similar to the behavior seen for usual cross-linked rubbers.[48−51] It is of interest to examine if this similarity holds *quantitatively*. For this purpose, we can compare the $\sigma_E$ data of the $(SIS)_p$ copolymers with a reliable molecular model for rubbers. Urayama et al.[49−51] utilized rubber samples prepared by end-cross-linking of prepolymers to demonstrate that among several models the Edwards−Vilgis slip-link model[52] most accurately describes the stress of the rubbers in various deformation modes (uniaxial and general biaxial deformation). Thus, we make the comparison with this model.

The Edwards−Vilgis model considers the rubber network containing trapped entanglements but no dangling loops/tails and represents these entanglements as the slip-links. The model describes the finite extensibility of the strands of the rubber network with respect to their primitive path and attributes the maximum stretch of the rubber to that of the *trapped entanglement segment*, not the network strand itself. The relationship between $\sigma_E$ and $\lambda$ deduced from the model is summarized in Appendix A. This relationship is written in terms of the equilibrium shear modulus, $G_e$ (given by eq 2 for our $(SIS)_p$ systems), and two parameters, $\eta$ and $\alpha$: $\eta$ represents the magnitude of the slippage of the slip-link, and $\alpha$ is a measure of the extensibility limit of the trapped entanglement segment; $\alpha = 1/\lambda_{max,ent}$ with $\lambda_{max,ent}$ being the maximum stretch ratio of

this segment. For usual unswollen rubbers, the $\alpha$ value is of the order of 0.1.[49−51]

In the concentrated I/C14 matrix in the $(SIS)_p$ multiblock systems, the trapped entanglement segment of the I blocks at equilibrium should have the unperturbed end-to-end distance, $R_e^\circ \propto M_e^{1/2}$. Thus, the $\lambda_{max,ent}$ value of this segment ($M_e = 19 \times 10^3$; cf. eq 5) is estimated to be

$$\lambda_{max,ent} = \frac{R_{e,max}}{R_e^\circ} = \frac{R_e^\circ}{b_K} \cong 12 \tag{13}$$

Here, $R_{e,max}$ ($=\{R_e^\circ\}^2/b_K = 137$ nm) and $b_K$ ($=0.93$ nm) are the full-stretch length of the trapped entanglement segment and the Kuhn length, respectively. The $R_e^\circ$ and $b_K$ values were taken from literature for linear *cis*-polyisoprene:[53] The unperturbed end-to-end distance is given by $R^\circ(M) = 0.082M^{1/2}$ nm and thus $R_e^\circ = 11.3$ nm for $M_e = 19 \times 10^3$.

For the corresponding $\alpha$ value ($=1/12.2 = 0.082$) and various $\eta$ values, we utilized the Edwards−Vilgis model to calculate the stress of the undecablock system. The result for $(\alpha, \eta) = (0.082, 5)$ is shown with the dotted curve in the top part of Figure 9. The calculated stress diverges at $\epsilon_{max} = \ln(1/\alpha) = 2.5$ and significantly deviates upward from the data at large $\epsilon$. The shape of the calculated curve changes moderately with the $\eta$ value, but the divergence at $\epsilon_{max} = 2.5$ occurs irrespective of the $\eta$ value. Thus, the undecablock system is more extensible than expected from the Edwards−Vilgis model. This result indicates that the behavior of the undecablock system is quantitatively different from the behavior of usual rubbers, the latter being well described by the model considering the stretch of the trapped entanglement segments.[54] This difference is discussed below in relation to the osmotic interaction in the $(SIS)_p$ multiblock systems.

**3.5. Origin of the High Extensibility of $(SIS)_p$ Systems.** In relation to the above difference, it is informative to examine the extensibility limit of the I blocks in the multiblock systems. Among all bridge-type I blocks, the I blocks connecting the closest-neighbor S domains (located at the corner and center of the bcc cell) have the smallest end-to-end distance $R_{I,b}$ at rest and are most extensible. Thus, the I blocks connecting these S domains should govern the extensional behavior at large $\epsilon$ seen in Figure 9. Although the bcc lattices seen for the $(SIS)_p$ systems are not of high coherence, we may estimate $R_{I,b}$ of such I blocks from the (average) cell edge length $a$ ($\cong$40 nm; cf. Figure 4) and the radius of the S domain $r_S$ ($=9.4$ nm) as

$$R_{I,b} = \frac{\sqrt{3}}{2}a - 2r_S \cong 15.8 \text{ nm} \tag{14}$$

(The $r_S$ value was calculated from the $a$ value and the volume fraction of the S blocks in the system, $v_S = 0.11$.) This $R_{I,b}$ agrees well with the unperturbed end-to-end distance of the I block, $R_I^\circ(M_I) = 0.082M_I^{1/2} \cong 16.4$ nm ($M_I \cong 40 \times 10^3$; cf. Table 1). Since the I blocks in the microphase-separated $(SIS)_p$ systems *at rest* would not be significantly stretched (beyond the unperturbed $R_I^\circ$), this agreement suggests that $R_{I,b}$ is satisfactorily estimated by eq 14.

From the full stretch length of the I block $R_{I,max}$ ($=\{R_I^\circ\}^2/b_K = 289$ nm)[53] and $R_{I,b}$ given in eq 14, the maximum stretch ratio of the bridge-type I block is estimated to be

$$\lambda_{I,b} = \frac{R_{I,max}}{R_{I,b}} \cong 18 \tag{15}$$

(The $\lambda_{I,b}$ value changes only a little even if we evaluate $\lambda_{I,b}$ as $R_{I,max}/R_I^\circ$.) As noted from eqs 12 and 15, individual I blocks are still less extensible compared to the undecablock system as a whole ($\lambda_{I,b} < \lambda_{max}$). However, the bcc cell in the system would be orientated in the stretch direction and thus the I blocks not orientated in this direction at rest would stretch as well as *rotate*. With this rotation, the projection of the end-to-end vector of the bridge-type I block in the stretch direction would become larger, *on average*, by a factor of $\lambda_{rot} = [\int_0^{\pi/2} \cos\theta \sin\theta \, d\theta / \int_0^{\pi/2} \sin\theta \, d\theta]^{-1} = 2$, where $\theta$ is an angle between the end-to-end vector of the I block at rest and the stretch direction. Then, for the I blocks connecting the closest-neighbor S domains, the *apparent* maximum stretch ratio including this *rotational contribution* is roughly estimated to be[55]

$$\lambda_{max,app} = \lambda_{rot}\lambda_{I,b} \cong 36 \tag{16}$$

This $\lambda_{max,app}$ value is close to the $\lambda_{max}$ value observed for the undecablock system (eq 12). Considering this result, we utilized $\alpha = 1/\lambda_{max} = 0.033$ and $\eta = 5$ in the Edwards−Vilgis model to calculate $\sigma_E$ for the undecablock and heptablock systems exhibiting the significant hardening. The results are shown with the solid curves in Figure 9.

In the $(SIS)_p$ systems, some I blocks have the dangling loop conformation and would not be largely stretched even under a large macroscopic extension. Furthermore, among the bridge-type I blocks, some should be already orientated in the stretch direction at rest and their $\lambda_{max}$ should not be contributed from the rotation. Such bridges can be stretched only up to $\lambda_{I,b}$ ($\cong$18; cf. eq 15), and a further stretch of the system unavoidably results in the pullout of the S blocks connected to these I blocks. In addition, the S domains would be anisotropically arranged in the system at large $\lambda$ but a change in the filler effect due to this anisotropic arrangement is not properly accounted in the $\sigma_E-\lambda$ relationship explained in Appendix A. For these reasons, no perfect agreement is expected between the calculated and measured $\sigma_E$. Nevertheless, a good agreement is seen in Figure 9: For the heptablock systems exhibiting the rupture at $\epsilon_{max} \cong 1.6$ ($\lambda_{max} \cong 5 < \lambda_{I,b}$), the calculated $\sigma_E$ (solid curves) agrees well with the data up to the rupture point. For the undecablock system, a considerable agreement is noted in a wider range of $\epsilon < 2.8$, i.e., in the range of $\lambda < 17 \cong \lambda_{I,b}$ where *all* bridge-type I blocks can sustain the stress unless the connected S blocks are pulled out.

This result and the close agreement of $\lambda_{max,app}$ (eq 16) and $\lambda_{max}$ (eq 12) suggest that the very high extensibility of the undecablock system is attributable to the full stretch of the bridge-type I block as a whole (not the trapped entanglement segment) as well as to the orientation of the bcc cell that results in the rotation of the I block. For the heptablock systems, the pull out of the PS blocks appears to have occurred before the I blocks were fully stretched thereby giving $\lambda_{max} < \lambda_{I,b}$. However, since the $\sigma_E$ data of the heptablock systems up to the rupture point are indistinguishable from the data of the undecablock system (and well described by the Edwards−Vilgis model with $\alpha = 1/\lambda_{max} = 0.033$), the I blocks in the heptablock systems would be able to fully stretch beyond the extensibility limit of the entanglement segment to sustain the stress *if* the connected S blocks were not pulled out. The situation seems to be the same for the penta- and triblock systems exhibiting the rupture at smaller $\lambda_{max}$.

Now, we need to consider how/why the bridge-type I blocks in the multiblock systems can be fully stretched to provide the systems with the high extensibility despite the trapped entanglement therein. Since the extensibility of usual rubbers is limited

by the trapped entanglement,[49−51] the high extensibility of the multiblock systems would be related to the osmotic interaction that is absent in the rubbers and possibly affects the trapped entanglement in the $(SIS)_p$ systems under a large stretch.

For this interaction, we note an interesting possibility. The macroscopic tension is not directly transmitted to the dangling loop-type I blocks. Thus, these loops should be just weakly stretched and exhibit the nonaffine deformation under a large, macroscopic deformation of the multiblock systems. Since the systems are incompressible and their width normal to the stretching direction decreases with increasing $\lambda$, the nonaffine deformation of the dangling loops results in an increase of the local I concentration near the S domains. Then, the end portion of the bridge-type I block near the S domains would be subjected to an *extra osmotic stretch* so as to reduce the concentration gradient. In fact, a related situation is known for a mixed polymer brush of long and short tethered chains:[56,57] The portion of the long chain near the tethered end is osmotically stretched by the short chains, and this stretch, being stronger than that in the absence of the short chains, enhances the repulsion between two mixed brush layers.

The extra osmotic stretch for the end portion of the bridge squeezes more segments to a middle portion of the bridge. These extra segments should effectively enlarge the molecular weight of the trapped entanglement segment under the macroscopic extension, and the maximum stretch ratio for the trapped entanglement in the case of full squeezing would coincide with $\lambda_{I,b}$ for the I block (eq 15), which possibly leads to the high extensibility seen for the multiblock systems containing the trapped entanglements.

From the above molecular picture, we expect that the extensibility and the mechanical toughness of the $(SIS)_p$ multiblock systems change with the loop/bridge population distribution. Specifically, the toughness *per bridge* would be enhanced when the loop population is increased while keeping the repeating unit number $p$. In this sense, the extensional behavior of the multiblock systems could be related to the dielectrically estimated bridge/loop fractions.

The molecular picture of the extra osmotic stretch for the end portion of the bridge has not been critically tested yet. The test can be achieved by externally tuning the bridge fraction $\phi_{bridge}$ in each $(SIS)_p$ system, quantifying the resulting change of $\phi_{bridge}$ with the dielectric method, and examining the effect of this change on the extensibility. This test is considered as an interesting subject of future work.

## 4. Concluding Remarks

For a series of symmetric $(SIS)_p$ multiblock copolymers having the inverted type-A dipole in a particular I block(s), we have examined the rheological and dielectric behavior in the I-selective solvent, *n*-tetradecane (C14). The $(SIS)_p$/C14 systems with the copolymer concentration of 40 wt % formed the bcc lattice of the S domains bridged by the I blocks to exhibit the gel-like elasticity.

The loop-type I blocks unequivocally coexist with the bridge-type I blocks. For the $(SIS)_p$/C14 systems, the dynamic behavior of the bridge-/loop-type I blocks having dipole inversion was examined from the $\epsilon''$ data that exclusively detected the fluctuation of the midpoint of these blocks. (The motion of the I block having noninverted dipole is dielectrically inert.) A moderate difference seen for the $\epsilon''$ data of the $(SIS)_p$ copolymers indicated that the bridge- and loop-type I blocks exhibit different dielectric responses and that the $\phi_{bridge}$ value changes moderately with the location of the dipole-inverted I block in the copolymer backbone as well as with the total block number.

This dielectric difference encouraged us to estimate $\phi_{bridge}$ from the $\epsilon''$ data of the $(SIS)_p$ and precursor SI copolymers (having the tail-type I block) on the basis the hypothesis of dielectric similarity between the loop and tail under the osmotic constraint. The $\phi_{bridge}$ estimated for the I block at the center of the copolymer backbone decreased slightly on an increase of the total block number, and $\phi_{bridge}$ was larger for the center I block than for the off-center I block. The decrease of $\phi_{bridge}$ of the center I block appeared to be related to an effect due to the finite length of the copolymer chains. The difference of $\phi_{bridge}$ for the center and off-center I blocks may have reflected an effect of the end S blocks (that can be more easily packed in the S domain compared to the longer, inner S block). These changes of $\phi_{bridge}$ deserve further studies.

In the uniaxial extension test, the $(SIS)_p$ systems exhibited a high extensibility associated with the strain hardening. Specifically, the undecablock system can be elongated to a surprisingly large stretch ratio, $\lambda_{max} \cong 30$. This high extensibility may reflect an extra stretch of the end portion of the bridge near the S domains due to the osmotic interaction with the coexisting loops. A test of this molecular picture is an interesting subject of future work.

**Acknowledgment.** Comments from Professor Kenji Urayama at Department of Material Chemistry, Kyoto University were helpful for improving the discussion of the extensional behavior of $(SIS)_p$. This work was partly supported by the Ministry of Education, Culture, and Sports, Science, and Technology, Japan (grant No. 17350108).

## Appendix A. Stress−Strain Relationship Deduced from the Edwards−Vilgis Model

For rubbers containing no dangling loop/tail, Edwards and Vilgis[52] derived a theoretical relationship between the uniaxial tensile force $f_E$ and stretch ratio $\lambda$. This relationship includes the link-slippage parameter $\eta$ and the extensibility parameter $\alpha$ as well as the number densities of the network strands and trapped entanglements, $N_c$ and $N_s$. For convenience of comparison with the extensional stress ($\sigma_E$) data of the $(SIS)_p$ multiblock systems, we rearranged the $f_E-\lambda$ relationship[52] into a relationship between $\sigma_E$ and $\lambda$ and utilized the equilibrium shear modulus $G_e$ as a parameter in the $\sigma_E-\lambda$ relationship. The results are summarized as

$$\frac{\sigma_E}{G_e} = \frac{f_c(\lambda;\alpha)}{g_c(\alpha) + \theta\, g_s(\alpha,\eta)} + \frac{f_{s1}(\lambda;\alpha,\eta) + f_{s2}(\lambda;\alpha) + f_{s3}(\lambda;\alpha,\eta) + f_{s4}(\lambda;\eta)}{\theta^{-1} g_c(\alpha) + g_s(\alpha,\eta)} \quad \text{(A1)}$$

with

$$G_e = F N_c k_B T \{g_c(\alpha) + \theta\, g_s(\alpha,\eta)\} \quad \text{(A2)}$$

Here, $\theta$ is a ratio of the number density of the slip-links (trapped entanglements) to that of the rubber strands. In eq A2, we have introduced the factor representing the filler effect in the $(SIS)_p$ systems, $F = 1 + 2.5\upsilon_S + 14.1\upsilon_S^2$ (=1.45 for the

volume fraction of the S domain $v_S = 0.11$). The functions $g$'s and $f$'s appearing in eqs A1 and A2 are defined below.

$$g_c(\alpha) = \frac{1 - 2\alpha^2 + 3\alpha^4}{(1 - 3\alpha^2)^2},$$

$$g_s(\alpha,\eta) = \frac{1 - (2 - 2\eta - 2\eta^2)\alpha^2 + (3 + 6\eta)\alpha^4}{(1 - 3\alpha^2)^2(1 + \eta)^2} \quad \text{(A3)}$$

$$f_c(\lambda;\alpha) = \frac{\{1 - 2\alpha^2 + \alpha^4(\lambda^2 + 2\lambda^{-1})\}}{\{1 - \alpha^2(\lambda^2 + 2\lambda^{-1})\}^2}(\lambda^2 - \lambda^{-1}) \quad \text{(A4)}$$

$$f_{s1}(\lambda;\alpha,\eta) = \frac{(1 - \alpha^2)\alpha^2(1 + \eta)}{\{1 - \alpha^2(\lambda^2 + 2\lambda^{-1})\}^2}\left(\frac{\lambda^2}{1 + \eta\lambda^2} + \frac{2}{\eta + \lambda}\right) \times (\lambda^2 - \lambda^{-1}) \quad \text{(A5)}$$

$$f_{s2}(\lambda;\alpha) = \frac{-\alpha^2}{\{1 - \alpha^2(\lambda^2 + 2\lambda^{-1})\}}(\lambda^2 - \lambda^{-1}) \quad \text{(A6)}$$

$$f_{s3}(\lambda;\alpha,\eta) = \frac{(1 - \alpha^2)(1 + \eta)}{\{1 - \alpha^2(\lambda^2 + 2\lambda^{-1})\}}\left\{\frac{\lambda^2}{(1 + \eta\lambda^2)^2} - \frac{\lambda}{(\eta + \lambda)^2}\right\} \quad \text{(A7)}$$

$$f_{s4}(\lambda;\eta) = \eta\left\{\frac{\lambda^2}{1 + \eta\lambda^2} - \frac{1}{\eta + \lambda}\right\} \quad \text{(A8)}$$

In the comparison with the $\sigma_E$ data of the $(SIS)_p$ systems, we utilized appropriately chosen $\alpha$ and $\eta$ values and the measured $G_e$ value (eq 2) in eqs A1 and A2 to calculate $\sigma_E$. The number density ratio $\theta$ was calculated from the values of $\alpha$, $\eta$, and $G_e$ as $\theta = \{(G_e/FN_c\, k_BT) - g_c(\alpha)\}/g_s(\alpha,\eta)$; cf. eq A2.

## References and Notes


(1) Matsushita, Y. *Macromolecules* **2007**, *40*, 771.
(2) Bates, F. F.; Fredrickson, G. H. *Annu. Rev. Chem. Phys.* **1990**, *41*, 525.
(3) Hamley, I. W. *The Physics of Block Copolymers*, Oxford Press: Oxford, U.K., 1998.
(4) Watanabe, H. Rheology of Multiphase Polymeric Systems. In *Structure and Properties of Multiphase Polymeric Materials*; Araki, T., Qui, T. C., Shibayama, M., Eds.; Marcel Dekker, New York, 1998; Chapter 9.
(5) Hashimoto, T.; Shibayama, M.; Kawai, H. *Macromolecules* **1980**, *13*, 1237.
(6) Tan, H.; Watanabe, H.; Matsumiya, Y.; Kanaya, T.; Takahashi, Y. *Macromolecules* **2003**, *36*, 2886.
(7) Wu, Li.; Cochran, E. W.; Lodge, T. P.; Bates, F. S. *Macromolecules* **2004**, *37*, 3360.
(8) Watanabe, H.; Sato, T.; Osaki, K. *Macromolecules* **2000**, *33*, 2545.
(9) Watanabe, H.; Kotaka, T. *J. Rheol.* **1983**, *27*, 223.
(10) Watanabe, H. *Acta Polym.* **1997**, *48*, 215.
(11) Watanabe, H.; Kanaya, T.; Takahashi, Y. *Macromolecules* **2001**, *34*, 662.
(12) Takano, A.; Kamaya, I.; Takahashi, Y.; Matsushita, Y. *Macromolecules* **2005**, *38*, 9718.
(13) Takahashi, Y.; Song, Y. H.; Nemoto, N.; Takano, A.; Akazawa, Y.; Matsushita, Y. *Macromolecules* **2005**, *38*, 9724.
(14) Sato, T.; Watanabe, H.; Osaki, K. *Macromolecules* **1996**, *29*, 6231.
(15) Watanabe, H.; Sato, T.; Osaki, K.; Yao, M. L.; Yamagishi, A. *Macromolecules* **1997**, *30*, 5877.
(16) Spontak, R. J.; Smith, S. D. *J. Polym. Sci., Part B: Polym. Phys.* **2001**, *39*, 947.
(17) Mori, Y.; Lim, L. S.; Bates, F. S. *Macromolecules* **2003**, *36*, 9879.
(18) Vigild, M. E.; Chu, C.; Sugiyama, M.; Chaffin, K. A.; Bates, F. S. *Macromolecules* **2001**, *34*, 951.
(19) Wu, Li.; Lodge, T. P.; Bates, F. S. *Macromolecules* **2004**, *37*, 8184.
(20) Wu, Li.; Lodge, T. P.; Bates, F. S. *Macromolecules* **2006**, *39*, 294.
(21) Matsushita, Y.; Mogi, Y.; Mukai, H.; Watanabe, J.; Noda, I. *Polymer* **1994**, *35*, 246.
(22) Nagata, Y.; Masuda, J.; Noda. A.; Cho, D.; Takano, A.; Matsushita, Y. *Macromolecules* **2005**, *38*, 10220.
(23) Ganesan, V.; Fredrickson, G. H. *J. Rheol.* **2001**, *45*, 161.
(24) Li, B. Q.; Ruckenstein, E. *Macromol. Theory Simul.* **1998**, *7*, 333.
(25) Watanabe, H. *Macromolecules* **1995**, *28*, 5006.
(26) Watanabe, H.; Tan, H. *Macromolecules* **2004**, *37*, 5118.
(27) Matsen, M. W. *J. Chem. Phys.* **1995**, *102*, 3884.
(28) Matsen, M. W.; Schick, M. *Macromolecules* **1994**, *27*, 187.
(29) Watanabe, H. *Prog. Polym. Sci.* **1999**, *24*, 1253.
(30) Watanabe, H.; Urakawa, O.; Kotaka, T. *Macromolecules* **1993**, *26*, 5073.
(31) Morton, M.; Fetters, L. J. *Rubber Chem. Technol.* **1975**, *48*, 359.
(32) Morton, M. *Anionic Polymerization: Principles and Practice*; Academic Press: New York, 1983.
(33) Fujimoto, T.; Nagasawa, M. *Advanced Techniques for Polymer Synthesis*; Kagaku-Dojin: Kyoto, Japan, 1972.
(34) Yoshida, H.; Watanabe, H.; Adachi, K.; Kotaka, T. *Macromolecules* **1991**, *24*, 2981.
(35) Matsumiya, Y.; Watanabe, H.; Osaki, K. *Macromolecules* **2000**, *33*, 499.
(36) Watanabe, H.; Matsumiya, Y.; Inoue, T. *Macromolecules* **2002**, *35*, 5702.
(37) Matsumiya, Y.; Matsumoto, M.; Watanabe, H.; Kanaya, T.; Takahashi, Y. *Macromolecules* **2007**, *40*, 3724.
(38) Guth, E. *J. Appl. Phys.* **1945**, *16*, 20.
(39) If we employ the dilution exponent of 1.3 (that gives $M_e = M_{e,bulk}/\varphi_1^{1.3}$), the $G_{e,ent}^\circ$ and $M_e$ values given in eqs 4 and 5 change to $3.3 \times 10^4$ Pa and $27 \times 10^3$, respectively. However, the argument of the trapped entanglement presented in this paper is not affected by these small changes of the $G_{e,ent}^\circ$ and $M_e$ values.
(40) Graessley, W. W. *Adv. Polym. Sci.* **1974**, *16*, 1.
(41) Watanabe, H.; Yamada, H.; Urakawa, O. *Macromolecules* **1995**, *28*, 6443.
(42) Watanabe, H.; Sato, T.; Osaki, K.; Matsumiya, Y.; Anastasiadis, S. H. *Nihon Reoroji Gakkaishi (J. Soc. Rheol. Jpn.)* **1999**, *27*, 173.
(43) Karatasos, K.; Anastasiadis, S. H.; Pakula, T.; Watanabe, H. *Macromolecules* **2000**, *33*, 523.
(44) Floudas, G.; Paraskeva, S.; Hadjichristidis, N.; Fytas, G.; Chu, B.; Semenov, A. N. *J. Chem. Phys.* **1997**, *107*, 5502.
(45) Karatasos, K.; Anastasiadis, S. H.; Floudas, G.; Fytas, G.; Pispas, S.; Hadjichristidis, N.; Pakula, T. *Macromolecules* **1996**, *29*, 1326.
(46) Obukhov, S. P.; Rubinstein, M.; Colby, R. H. *Macromolecules* **1994**, *27*, 3191.
(47) Urayama, K.; Kohjiya, S. *Eur. Phys. J. B* **1998**, *2*, 75.
(48) Strobl, G. *The Physics of Polymers*, 3rd ed.; Springer: Berlin, 2007.
(49) Urayama, K.; Kawamura, T.; Kohjiya, S. *Macromolecules* **2003**, *34*, 8621.
(50) Urayama, K.; Kawamura, T.; Kohjiya, S. *J. Chem. Phys.* **2003**, *118*, 5658.
(51) Urayama, K. *Nihon Reoroji Gakkaishi (J. Soc. Rheol. Jpn.)* **2005**, *33*, 257.
(52) Edwards, S. F.; Vilgis, T. *Polymer* **1986**, *27*, 483.
(53) Fetters, L. J.; Lohse, D. J.; Colby, R. H. Chain Dimension and Entanglement Spacing. In *Physical Properties of Polymers Handbook*, 2nd ed.; Mark, J. E., Ed.; Springer: New York 2007.
(54) Figure 9 demonstrates a difference between the $\sigma_E$ data for the undecablock system (circles and squares) and the stress due to the bridges $\sigma_{E,bridge}$ calculated from the Edwards−Vilgis model (with $\alpha = 0.082$; dotted curve in Figure 9). One may attribute this difference to the stress due to the loops, $\sigma_{E,loop}$, and argue a necessity of comparing the data with the calculated $\sigma_E = \sigma_{E,bridge} + \sigma_{E,loop}$. However, with any choice of the loop stress, e.g., either a Hookean $\sigma_{E,loop}$ ($\propto\epsilon$) or $\sigma_{E,loop} = 0$, the calculated $\sigma_E$ significantly deviated from the data at large $\epsilon$ as long as $\sigma_{E,bridge}$ was calculated from the model with $\alpha = 0.082$.
(55) The $\lambda_{max,app}$ value ($\cong$36) given in eq 16 was estimated without consideration of effects of the glassy S domains. Thus, this value is to be regarded as a rough estimate.
(56) Dan, N.; Tirrell, M. *Macromolecules* **1993**, *26*, 6467.
(57) Dhoot, S.; Watanabe, H.; Tirrell, M. *Colloids Surf. A* **1994**, *86*, 47.


MA0712495